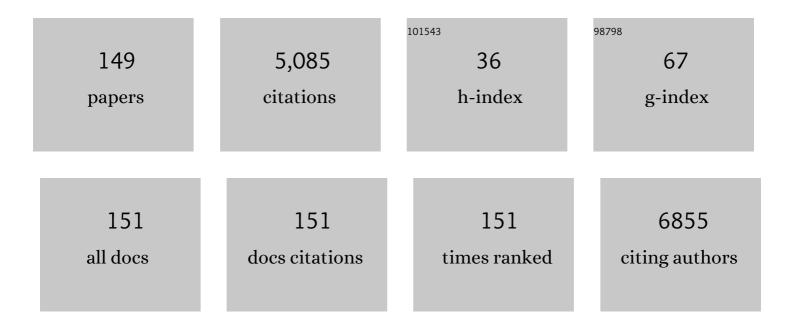
## List of Publications by Year in descending order

Source: https://exaly.com/author-pdf/5046104/publications.pdf Version: 2024-02-01



KEUL HENO

#	Article	IF	CITATIONS
1	Mist chemical vapor deposition of crystalline MoS <sub>2</sub> atomic layer films using sequential mist supply mode and its application in field-effect transistors. Nanotechnology, 2022, 33, 045601.	2.6	6
2	Quantitative Determination of Contradictory Bandgap Values of Bulk PdSe <sub>2</sub> from Electrical Transport Properties. Advanced Functional Materials, 2022, 32, 2108061.	14.9	11
3	Photoâ€Induced Tellurium Segregation in MoTe <sub>2</sub> . Physica Status Solidi - Rapid Research Letters, 2022, 16, .	2.4	10
4	Mist chemical vapor deposition of Al <sub>1â^'<i>x</i></sub> Ti <i><sub>x</sub></i> O <i><sub>y</sub></i> thin films and their application to a high dielectric material. Journal of Applied Physics, 2022, 131, 105301.	2.5	2
5	Ultrafast Operation of 2D Heterostructured Nonvolatile Memory Devices Provided by the Strong Short-Time Dielectric Breakdown Strength of <i>h</i> -BN. ACS Applied Materials & Interfaces, 2022, 14, 25659-25669.	8.0	4
6	Reversible Chargeâ€Polarity Control for Multioperationâ€Mode Transistors Based on van der Waals Heterostructures. Advanced Science, 2022, 9, .	11.2	6
7	Enhanced Exciton–Exciton Collisions in an Ultraflat Monolayer MoSe <sub>2</sub> Prepared through Deterministic Flattening. ACS Nano, 2021, 15, 1370-1377.	14.6	9
8	AlO <sub><i>x</i></sub> Thin Films Synthesized by Mist Chemical Vapor Deposition, Monitored by a Fast-Scanning Mobility Particle Analyzer, and Applied as a Gate Insulating Layer in the Field-Effect Transistors. ACS Applied Electronic Materials, 2021, 3, 658-667.	4.3	4
9	State-of-the-Art of Solution-Processed Crystalline Silicon/Organic Heterojunction Solar Cells: Challenges and Future. Challenges and Advances in Computational Chemistry and Physics, 2021, , 33-56.	0.6	1
10	Material and Device Structure Designs for 2D Memory Devices Based on the Floating Gate Voltage Trajectory. ACS Nano, 2021, 15, 6658-6668.	14.6	16
11	Intrinsic Electronic Transport Properties and Carrier Densities in PtS <sub>2</sub> and SnSe <sub>2</sub> : Exploration of n <sup>+</sup> â€Source for 2D Tunnel FETs. Advanced Electronic Materials, 2021, 7, 2100292.	5.1	8
12	Twist Angle-Dependent Interlayer Exciton Lifetimes in van der Waals Heterostructures. Physical Review Letters, 2021, 126, 047401.	7.8	88
13	Low-temperature growth of crystalline tungsten disulfide thin films by using organic liquid precursors. Japanese Journal of Applied Physics, 2020, 59, SCCC04.	1.5	4
14	Improved efficiency of methylammonium-free perovskite thin film solar cells by fluorinated ammonium iodide treatment. Organic Electronics, 2020, 78, 105596.	2.6	15
15	Self-assembled Fluorinated Polymer Passivation Layer for Efficient Perovskite Thin-film Solar Cells. Chemistry Letters, 2020, 49, 87-90.	1.3	6
16	All 2D Heterostructure Tunnel Field-Effect Transistors: Impact of Band Alignment and Heterointerface Quality. ACS Applied Materials & Interfaces, 2020, 12, 51598-51606.	8.0	35
17	Effect of thermally annealed atomic-layer-deposited AlOx/chemical tunnel oxide stack layer at the PEDOT:PSS/n-type Si interface to improve its junction quality. Journal of Applied Physics, 2020, 128, 045305.	2.5	3
18	Facile and Reversible Carrier-Type Manipulation of Layered MoTe <sub>2</sub> Toward Long-Term Stable Electronics. ACS Applied Materials & Interfaces, 2020, 12, 42918-42924.	8.0	4

#	Article	IF	CITATIONS
19	Excition diffusion in <mmi:math xmlns:mml="http://www.w3.org/1998/Math/MathML"&gt; <mml:mrow> <mml:mi> h </mml:mi> <mml:mi> BN </mml:mi> -encapsulated monolayer <mml:math xmlns:mml="http://www.w3.org/1998/Math/MathML"&gt; <mml:mrow> <mml:mi> Mo </mml:mi> <mml:msub> <mml:m Blowtine Bactow B. 2020, 202</mml:m </mml:msub></mml:mrow></mml:math </mml:mrow></mmi:math 	3.2	12
20	Understanding the Memory Window Overestimation of 2D Materials Based Floating Gate Type Memory Devices by Measuring Floating Gate Voltage. Small, 2020, 16, e2004907.	10.0	11
21	Synthesis of AlO <i>x</i> thin films by atmospheric-pressure mist chemical vapor deposition for surface passivation and electrical insulator layers. Journal of Vacuum Science and Technology A: Vacuum, Surfaces and Films, 2020, 38, .	2.1	4
22	Ultrafast dynamics of the low frequency shear phonon in $1T\hat{a}$ €²-MoTe2. Applied Physics Letters, 2020, 116, .	3.3	21
23	Flat bands in twisted bilayer transition metal dichalcogenides. Nature Physics, 2020, 16, 1093-1096.	16.7	197
24	Investigation of laser-induced-metal phase of MoTe <sub>2</sub> and its contact property via scanning gate microscopy. Nanotechnology, 2020, 31, 205205.	2.6	11
25	Role of the solvent in large crystal grain growth of inorganic-organic halide FA0.8Cs0.2Pbl <i>x</i> Br3 â` <i>x</i> perovskite thin films monitored by ellipsometry. Journal of Vacuum Science and Technology B:Nanotechnology and Microelectronics, 2019, 37, .	1.2	2
26	Barrier Formation at the Contacts of Vanadium Dioxide and Transition-Metal Dichalcogenides. ACS Applied Materials & Interfaces, 2019, 11, 36871-36879.	8.0	9
27	Exciton Diffusion in hBN-encapsulated Monolayer MoSe2. , 2019, , .		0
28	Highly crystalline large-grained perovskite films using two additives without an antisolvent for high-efficiency solar cells. Thin Solid Films, 2019, 679, 27-34.	1.8	7
29	Oxygen-Sensitive Layered MoTe <sub>2</sub> Channels for Environmental Detection. ACS Applied Materials & Interfaces, 2019, 11, 47047-47053.	8.0	13
30	Selective oxidation of the surface layer of bilayer WSe <sub>2</sub> by laser heating. Japanese Journal of Applied Physics, 2019, 58, 120903.	1.5	6
31	Site-dependence of relationships between photoluminescence and applied electric field in monolayer and bilayer molybdenum disulfide. Japanese Journal of Applied Physics, 2019, 58, 015001.	1.5	1
32	Gate-Tunable Thermal Metal–Insulator Transition in VO <sub>2</sub> Monolithically Integrated into a WSe <sub>2</sub> Field-Effect Transistor. ACS Applied Materials & Interfaces, 2019, 11, 3224-3230.	8.0	29
33	Reversible and Precisely Controllable p/nâ€Type Doping of MoTe <sub>2</sub> Transistors through Electrothermal Doping. Advanced Materials, 2018, 30, e1706995.	21.0	68
34	Optical Anisotropy and Compositional Ratio of Conductive Polymer PEDOT:PSS and Their Effect on Photovoltaic Performance of Crystalline Silicon/Organic Heterojunction Solar Cells. , 2018, , 137-159.		4
35	Pronounced photogating effect in atomically thin WSe2 with a self-limiting surface oxide layer. Applied Physics Letters, 2018, 112, .	3.3	38
36	Ultrathin Bismuth Film on 1T-TaS <sub>2</sub> : Structural Transition and Charge-Density-Wave Proximity Effect. Nano Letters, 2018, 18, 3235-3240.	9.1	28

#	Article	IF	CITATIONS
37	Self-passivated ultra-thin SnS layers <i>via</i> mechanical exfoliation and post-oxidation. Nanoscale, 2018, 10, 22474-22483.	5.6	42
38	Fabrication of [CH(NH <sub>2</sub> ) <sub>2</sub> ] <sub>0.8</sub> Cs <sub>0.2</sub> PbI <sub>3</sub> Perovskite Thin Films for n-i-p Planar-structure Solar Cells by a One-step Method Using 1-Cyclohexyl-2-pyrrolidone as an Additive. Chemistry Letters, 2018, 47, 905-908.	1.3	7
39	2D Tunnel Field Effect Transistors (FETs) with a Stable Chargeâ€Transferâ€Type p <sup>+</sup> â€WSe <sub>2</sub> Source. Advanced Electronic Materials, 2018, 4, 1800207.	5.1	41
40	Fabrication and Surface Engineering of Two-Dimensional SnS Toward Piezoelectric Nanogenerator Application. MRS Advances, 2018, 3, 2809-2814.	0.9	19
41	Anisotropic band splitting in monolayer NbSe2: implications for superconductivity and charge density wave. Npj 2D Materials and Applications, 2018, 2, .	7.9	43
42	Fabrication of {CH(NH <sub>2</sub> ) <sub>2</sub> } <sub>1â^²</sub> <i><sub>x</sub></i> Cs <i><sub>x</sub></i> PbI <sub>3<!--<br-->Perovskite Thin Films by Two-step Method and Its Application to Thin Film Solar Cells. Chemistry Letters, 2017, 46, 612-615.</sub>	sub> 1.3	5
43	Sensitive Phonon-Based Probe for Structure Identification of 1T′ MoTe <sub>2</sub> . Journal of the American Chemical Society, 2017, 139, 8396-8399.	13.7	46
44	Barium hydroxide hole blocking layer for front- and back-organic/crystalline Si heterojunction solar cells. Journal of Applied Physics, 2017, 122, .	2.5	26
45	Exfoliation and van der Waals heterostructure assembly of intercalated ferromagnet Cr <sub>1/3</sub> TaS <sub>2</sub> . 2D Materials, 2017, 4, 041007.	4.4	41
46	Effect of substrate bias on mist deposition of conjugated polymer on textured crystallineâ€Si for efficient câ€Si/organic heterojunction solar cells. Physica Status Solidi (A) Applications and Materials Science, 2016, 213, 1922-1925.	1.8	8
47	Monolayer 1T-NbSe2 as a Mott insulator. NPG Asia Materials, 2016, 8, e321-e321.	7.9	109
48	Correlation between the fine structure of spin-coated PEDOT:PSS and the photovoltaic performance of organic/crystalline-silicon heterojunction solar cells. Journal of Applied Physics, 2016, 120, .	2.5	46
49	Carrier Polarity Control in α-MoTe <sub>2</sub> Schottky Junctions Based on Weak Fermi-Level Pinning. ACS Applied Materials & Interfaces, 2016, 8, 14732-14739.	8.0	72
50	Investigating the chemical mist deposition technique for poly(3,4-ethylenedioxythiophene):poly(styrene sulfonate) on textured crystalline-silicon for organic/crystalline-silicon heterojunction solar cells. Japanese Journal of Applied Physics, 2016, 55, 031601.	1.5	16
51	Synthesis of Highâ€Quality Largeâ€Area Homogenous 1T′ MoTe <sub>2</sub> from Chemical Vapor Deposition. Advanced Materials, 2016, 28, 9526-9531.	21.0	125
52	Nafion-Modified PEDOT:PSS as a Transparent Hole-Transporting Layer for High-Performance Crystalline-Si/Organic Heterojunction Solar Cells with Improved Light Soaking Stability. ACS Applied Materials & Interfaces, 2016, 8, 31926-31934.	8.0	63
53	Role of Isopropyl Alcohol Solvent in the Synthesis of Organic–Inorganic Halide CH(NH <sub>2</sub> ) <sub>2</sub> PbI <sub><i>x</i>/i&gt;</sub> Br <sub>3–<i>x</i></sub> Perovskite Thin Films by a Two-Step Method. Journal of Physical Chemistry C, 2016, 120, 25371-25377.	3.1	12
54	Solution-processed crystalline silicon double-heterojunction solar cells. Applied Physics Express, 2016. 9. 022301.	2.4	15

#	Article	IF	CITATIONS
55	Self-Limiting Oxides on WSe <sub>2</sub> as Controlled Surface Acceptors and Low-Resistance Hole Contacts. Nano Letters, 2016, 16, 2720-2727.	9.1	131
56	Introduction to the Growth of Bulk Single Crystals of Two-Dimensional Transition-Metal Dichalcogenides. Journal of the Physical Society of Japan, 2015, 84, 121015.	1.6	36
57	Highly Efficient Solutionâ€Processed Poly(3,4â€ethylenedioâ€xythiophene):Poly(styrenesulfonate)/Crystalline–Silicon Heterojunction Solar Cells with Improved Lightâ€Induced Stability. Advanced Energy Materials, 2015, 5, 1500744.	19.5	85
58	Origin of Noise in Layered MoTe <sub>2</sub> Transistors and its Possible Use for Environmental Sensors. Advanced Materials, 2015, 27, 6612-6619.	21.0	72
59	Solution-Processed Organic/Crystalline-Silicon Heterojunction Solar Cells with Improved Light-Induced Stability. , 2015, , .		0
60	Electrostatically Reversible Polarity of Ambipolar α-MoTe <sub>2</sub> Transistors. ACS Nano, 2015, 9, 5976-5983.	14.6	113
61	van der Waals junctions of layered 2D materials for functional devices. , 2015, , .		0
62	Self-Limiting Layer-by-Layer Oxidation of Atomically Thin WSe <sub>2</sub> . Nano Letters, 2015, 15, 2067-2073.	9.1	204
63	Double resonance Raman modes in monolayer and few-layer <mml:math xmlns:mml="http://www.w3.org/1998/Math/MathML"&gt;<mml:msub><mml:mi mathvariant="normal"&gt;MoTe<mml:mn>2</mml:mn></mml:mi </mml:msub>. Physical Review B. 2015. 91</mml:math 	3.2	99
64	Changes in structure and chemical composition of α-MoTe <sub>2</sub> and β-MoTe <sub>2</sub> during heating in vacuum conditions. Applied Physics Express, 2015, 8, 095201.	2.4	36
65	Large-Area Synthesis of High-Quality Uniform Few-Layer MoTe <sub>2</sub> . Journal of the American Chemical Society, 2015, 137, 11892-11895.	13.7	302
66	Construction of van der Waals magnetic tunnel junction using ferromagnetic layered dichalcogenide. Applied Physics Letters, 2015, 107, .	3.3	47
67	Efficient organic/polycrystalline silicon hybrid solar cells. Nano Energy, 2015, 11, 260-266.	16.0	18
68	Fabrication of Organic/inorganic Hybrid CMOS Devices using Solution-processed Graphene Electrodes. IEEJ Transactions on Electronics, Information and Systems, 2015, 135, 156-159.	0.2	0
69	Improved performance of poly(3,4-ethylenedioxythiophene):poly(stylene sulfonate)/n-Si hybrid solar cell by incorporating silver nanoparticles. Japanese Journal of Applied Physics, 2014, 53, 110305.	1.5	7
70	Ambipolar MoTe <sub>2</sub> Transistors and Their Applications in Logic Circuits. Advanced Materials, 2014, 26, 3263-3269.	21.0	388
71	Real-time measurement of optical anisotropy during film growth using a chemical mist deposition of poly(3,4-ethylenedioxythiophene):poly(styrenesulfonate). Journal of Applied Physics, 2014, 115, 123514.	2.5	9
72	Self-assembled silver nanowires as top electrode for poly(3,4-ethylenedioxythiophene):poly(stylenesulfonate)/n-silicon solar cell. Thin Solid Films, 2014, 558, 306-310.	1.8	16

#	Article	IF	CITATIONS
73	Improved photovoltaic response by incorporating green tea modified multiwalled carbon nanotubes in organic–inorganic hybrid solar cell. Canadian Journal of Physics, 2014, 92, 849-852.	1.1	2
74	Self assembled silver nanowire mesh as top electrode for organic–inorganic hybrid solar cell. Canadian Journal of Physics, 2014, 92, 867-870.	1.1	7
75	Strong Enhancement of Raman Scattering from a Bulk-Inactive Vibrational Mode in Few-Layer MoTe <sub>2</sub> . ACS Nano, 2014, 8, 3895-3903.	14.6	275
76	High-performance top-gated monolayer SnS2 field-effect transistors and their integrated logic circuits. Nanoscale, 2013, 5, 9666.	5.6	269
77	Green-tea modified multiwalled carbon nanotubes for efficient poly(3,4-ethylenedioxythiophene):poly(stylenesulfonate)/n-silicon hybrid solar cell. Applied Physics Letters, 2013, 102, .	3.3	31
78	Efficient Organic Photovoltaic Cells Using MoO3Hole-Transporting Layers Prepared by Simple Spin-Cast of Its Dispersion Solution in Methanol. Japanese Journal of Applied Physics, 2013, 52, 020202.	1.5	4
79	Optical anisotropy in solvent-modified poly(3,4-ethylenedioxythiophene):poly(styrenesulfonic acid) and its effect on the photovoltaic performance of crystalline silicon/organic heterojunction solar cells. Applied Physics Letters, 2013, 102, .	3.3	43
80	Optical and carrier transport properties of graphene oxide based crystalline-Si/organic Schottky junction solar cells. Journal of Applied Physics, 2013, 114, .	2.5	4
81	Improved photovoltaic performance of crystalline-Si/organic Schottky junction solar cells using ferroelectric polymers. Applied Physics Letters, 2013, 103, .	3.3	24
82	Effects of molybdenum oxide molecular doping on the chemical structure of poly(3,4-ethylenedioxythiophene):poly(stylenesulfonate) and on carrier collection efficiency of silicon/poly(3,4-ethylenedioxythiophene):poly(stylenesulfonate) heterojunction solar cells. Applied Physics Letters, 2013, 102, 183503.	3.3	22
83	Top-Contacted Organic Field-Effect Transistors with Graphene Electrodes Prepared by Laminate Transfer Method. Applied Physics Express, 2012, 5, 125104.	2.4	2
84	Electrospray Deposition of Poly(3-hexylthiophene) Films for Crystalline Silicon/Organic Hybrid Junction Solar Cells. Japanese Journal of Applied Physics, 2012, 51, 061602.	1.5	5
85	Efficient Crystalline Si/Poly(ethylene dioxythiophene):Poly(styrene sulfonate):Graphene Oxide Composite Heterojunction Solar Cells. Applied Physics Express, 2012, 5, 032301.	2.4	28
86	Increased Organic Photovoltaic Cell Efficiency by Incorporating a Nonionic Fluorinated Surfactant Cathode Interlayer. Applied Physics Express, 2012, 5, 121601.	2.4	0
87	lonic liquid-mediated epitaxy of high-quality C60 crystallites in a vacuum. CrystEngComm, 2012, 14, 4939.	2.6	24
88	Crystalline Silicon/Graphene Oxide Hybrid Junction Solar Cells. Japanese Journal of Applied Physics, 2012, 51, 10NE22.	1.5	1
89	Electrospray-Deposited Poly(3,4-ethylenedioxythiophene):Poly(styrene sulfonate) for Poly(3-hexylthiophene):Phenyl-C\$_{61}\$-Butyric Acid Methyl Ester Photovoltaic Cells. Japanese Journal of Applied Physics, 2012, 51, 10NE30.	1.5	6
90	Optical properties and carrier transport in c-Si/conductive PEDOT:PSS(GO) composite heterojunctions. Physica Status Solidi C: Current Topics in Solid State Physics, 2012, 9, 2075-2078.	0.8	13

#	Article	IF	CITATIONS
91	Efficient crystalline Si/organic hybrid heterojunction solar cells. Physica Status Solidi C: Current Topics in Solid State Physics, 2012, 9, 2101-2106.	0.8	8
92	Chemical mist deposition of graphene oxide and PEDOT:PSS films for crystalline Si/organic heterojunction solar cells. Physica Status Solidi C: Current Topics in Solid State Physics, 2012, 9, 2134-2137.	0.8	22
93	Real-time ellipsometric characterization of the initial growth stage of poly(3,4-ethylenedioxythiophene):poly(styrene sulfonate) films by electrospray deposition using N,N-dimethylformamide solvent solution. Journal of Non-Crystalline Solids, 2012, 358, 2520-2524.	3.1	8
94	Highly efficient crystalline silicon/Zonyl fluorosurfactant-treated organic heterojunction solar cells. Applied Physics Letters, 2012, 100, .	3.3	102
95	Electrospray Deposition of Poly(3-hexylthiophene) Films for Crystalline Silicon/Organic Hybrid Junction Solar Cells. Japanese Journal of Applied Physics, 2012, 51, 061602.	1.5	4
96	Crystalline Silicon/Graphene Oxide Hybrid Junction Solar Cells. Japanese Journal of Applied Physics, 2012, 51, 10NE22.	1.5	5
97	Electrospray-Deposited Poly(3,4-ethylenedioxythiophene):Poly(styrene sulfonate) for Poly(3-hexylthiophene):Phenyl-C61-Butyric Acid Methyl Ester Photovoltaic Cells. Japanese Journal of Applied Physics, 2012, 51, 10NE30.	1.5	3
98	Fabrication of Transparent and Flexible Organic Field-Effect Transistors with Solution-Processed Graphene Source–Drain and Gate Electrodes. Applied Physics Express, 2011, 4, 021603.	2.4	31
99	Bulk heterojunction organic photovoltaic cell fabricated by the electrospray deposition method using mixed organic solvent. Physica Status Solidi - Rapid Research Letters, 2011, 5, 229-231.	2.4	45
100	Depth profile characterization of spin-coated poly(3,4-ethylenedioxythiophene): poly(styrene sulfonic) Tj ETQq0 0 State Physics, 2011, 8, 3025-3028.	0 rgBT /Ov 0.8	verlock 10 7 3
101	Atmospheric-pressure argon plasma etching of spin-coated 3,4-polyethylenedioxythiophene:polystyrenesulfonic acid (PEDOT:PSS) films for cupper phtalocyanine (CuPc)/C60 heterojunction thin-film solar cells. Thin Solid Films, 2011, 519, 6834-6839.	1.8	12
102	Real-Time Ellipsometric Characterization of Initial Growth Stage of Poly(3,4-ethylene) Tj ETQq0 0 0 rgBT /Overlock Applied Physics, 2011, 50, 081603.	10 Tf 50 3 1.5	307 Td (dio) 7
103	Depth Profile Characterization of Spin-Coated Poly(3,4-ethylenedioxythiophene):Poly(styrene sulfonic) Tj ETQq1 1 Japanese Journal of Applied Physics, 2011, 50, 08JG02.	0.784314 1.5	FrgBT /Over 2
104	Efficient Organic Photovoltaic Cells Using Hole-Transporting MoO3Buffer Layers Converted from Solution-Processed MoS2Films. Japanese Journal of Applied Physics, 2011, 50, 071604.	1.5	11
105	Surface Modification of Poly(3,4-ethylene dioxthiophene):Poly(styrene sulfonic acid) (PEDOT:PSS) Films by Atmospheric-Pressure Argon Plasma for Organic Thin-Film Solar Cells. Journal of Nanoscience and Nanotechnology, 2011, 11, 8035-8039.	0.9	1
106	Real-Time Ellipsometric Characterization of Initial Growth Stage of Poly(3,4-ethylene) Tj ETQq0 0 0 rgBT /Overlock Applied Physics, 2011, 50, 081603.	10 Tf 50 1 1.5	147 Td (dio) 2
107	Real-Time Ellipsometric Characterization of the Initial Growth Stage of Poly(3,4-ethylene) Tj ETQq1 1 0.784314 rgl and Nanotechnology, 2011, 11, 8030-8034.	3T /Overloo 0.9	ck 10 Tf 50 4
108	Origin of the ambipolar operation of a pentacene field-effect transistor fabricated on a poly(vinyl) Tj ETQq0 0 0 rgl	BT /Overloo 3.3	ck 10 Tf 50 29

94, 083305.

#	Article	IF	CITATIONS
109	Nucleation on the substrate surfaces during liquid flux-mediated vacuum deposition of rubrene. Journal of Crystal Growth, 2008, 311, 163-166.	1.5	7
110	Nanotransfer of the Polythiophene Molecular Alignment onto the Step-Bunched Vicinal Si(111) Substrate. Langmuir, 2008, 24, 11605-11610.	3.5	11
111	Molecular Layer-by-Layer Growth of C <sub>60</sub> Thin Films by Continuous-Wave Infrared Laser Deposition. Applied Physics Express, 2008, 1, 015005.	2.4	39
112	Step-bunched Bi-terminated Si(111) surfaces as a nanoscale orientation template for quasisingle crystalline epitaxial growth of thin film phase pentacene. Applied Physics Letters, 2008, 93, 223303.	3.3	15
113	Effect of Organic Buffer Layer on Performance of Pentacene Field-Effect Transistor Fabricated on Natural Mica Gate Dielectric. Japanese Journal of Applied Physics, 2007, 46, L913-L916.	1.5	9
114	Anisotropic Polymerization of a Long-Chain Diacetylene Derivative Langmuirâ^'Blodgett Film on a Step-Bunched SiO2/Si Surface. Langmuir, 2006, 22, 5742-5747.	3.5	7
115	Structure of Organic Thin Films Grown on Surface-modified Tantalum Oxide. Chemistry Letters, 2006, 35, 746-747.	1.3	2
116	Fabrication of an Organic Field-effect Transistor on a Mica Gate Dielectric. Chemistry Letters, 2006, 35, 354-355.	1.3	10
117	In-situ measurement of molecular orientation of the pentacene ultrathin films grown on SiO2 substrates. Surface Science, 2006, 600, 2518-2522.	1.9	27
118	Orientation Control of Standing Epitaxial Pentacene Monolayers Using Surface Steps and In-plane Band Dispersion Analysis by Angle Resolved Photoelectron Spectroscopy. Materials Research Society Symposia Proceedings, 2006, 965, 1.	0.1	3
119	Anodization of electrolytically polished Ta surfaces for enhancement of carrier injection into organic field-effect transistors. Journal of Applied Physics, 2005, 98, 114503.	2.5	26
120	Bulk-like pentacene epitaxial films on hydrogen-terminated Si(111). Applied Physics Letters, 2005, 87, 061917.	3.3	23
121	Scanning Tunneling Microscopy and Spectroscopy Study of LiBr/Si(001) Heterostructure. Japanese Journal of Applied Physics, 2004, 43, L203-L205.	1.5	3
122	Methyl-terminated Si(111) surface as the ultra thin protection layer to fabricate position-controlled alkyl SAMs by using atomic force microscope anodic oxidation. Surface Science, 2004, 552, 46-52.	1.9	11
123	Visible light photoemission and negative electron affinity of single-crystalline CsCl thin films. Surface Science, 2003, 544, 220-226.	1.9	12
124	Accumulation and Depletion Layer Thicknesses in Organic Field Effect Transistors. Japanese Journal of Applied Physics, 2003, 42, L1408-L1410.	1.5	105
125	Nano-scale anodic oxidation on a Si() surface terminated by bilayer-GaSe. Surface Science, 2002, 514, 27-32.	1.9	9
126	Low-energy electron energy loss spectroscopy of monolayer and thick La@C[sub 82] films grown on MoS[sub 2] substrates. AIP Conference Proceedings, 2001, , .	0.4	0

#	Article	IF	CITATIONS
127	Electron-energy-loss spectroscopy of KxC60 and K-halides: comparison in the K3p excitation region. Applied Surface Science, 2001, 169-170, 184-187.	6.1	4
128	Fabrication of GaAs Quantum Dots on a Bilayer-GaSe Terminated Si(111) Substrate. Japanese Journal of Applied Physics, 2001, 40, 1888-1891.	1.5	13
129	Investigation of the growth mechanism of an InSe epitaxial layer on a MoS2 substrate. Journal of Crystal Growth, 2000, 219, 115-122.	1.5	28
130	Comparative Study on Surfaces of Single-Crystalline Substrates. From Dielectric Substance to Semiconductor and Metal. Layered Material Substrates Hyomen Kagaku, 2000, 21, 716-723.	0.0	0
131	Highly sensitive reflection high-energy electron diffraction measurement by use of micro-channel imaging plate. Review of Scientific Instruments, 2000, 71, 3478-3479.	1.3	15
132	A Novel Method to Fabricate a Molecular Quantum Structure: Selective Growth of C60on Layered Material Heterostructures. Japanese Journal of Applied Physics, 1999, 38, 511-514.	1.5	15
133	Fabrication of C60 nanostructures by selective growth on GaSe/MoS2 and InSe/MoS2 heterostructure substrates. Applied Surface Science, 1998, 130-132, 670-675.	6.1	7
134	Fabrication of Molecular Crystal Nanostructures by a Selective Growth Method Hyomen Kagaku, 1998, 19, 14-20.	0.0	2
135	Nanostructure Fabrication Using Selective Growth on Nanosize Patterns Drawn by a Scanning Probe Microscope. Japanese Journal of Applied Physics, 1997, 36, 4061-4064.	1.5	10
136	Nanostructure fabrication by selective growth of molecular crystals on layered material substrates. Applied Physics Letters, 1997, 70, 1104-1106.	3.3	18
137	Investigation of the growth mechanism of layered semiconductor GaSe. Applied Surface Science, 1997, 113-114, 38-42.	6.1	34
138	Preparation of GaS Thin Films by Molecular Beam Epitaxy. Japanese Journal of Applied Physics, 1996, 35, L568-L570.	1.5	8
139	Scanning Tunneling Microscope Observation of the Metal-Adsorbed Layered Semiconductor Surfaces. Japanese Journal of Applied Physics, 1995, 34, 3342-4445.	1.5	7
140	Heteroepitaxial Growth of Layered GaSe Films on GaAs(001) Surfaces. Japanese Journal of Applied Physics, 1993, 32, L1444-L1447.	1.5	14
141	Heteroepitaxial Growth of Layered Semiconductor GaSe on a Hydrogen-Terminated Si(111) Surface*. Japanese Journal of Applied Physics, 1993, 32, L434-L437.	1.5	47
142	Hetero-epitaxy of layered compound semiconductor GaSe onto GaAs surfaces for very effective passivation of nanometer structures. Surface Science, 1992, 267, 43-46.	1.9	30
143	Heteroepitaxial growth by Van der Waals interaction in one-, two- and three-dimensional materials. Journal of Crystal Growth, 1991, 111, 1029-1032.	1.5	74
144	Heteroepitaxy of Layered Semiconductor GaSe on a GaAs(111)B Surface. Japanese Journal of Applied Physics, 1991, 30, L1352-L1354.	1.5	63

#	Article	IF	CITATIONS
145	Epitaxial growth of transition metal dichalcogenides on cleaved faces of mica. Journal of Vacuum Science and Technology A: Vacuum, Surfaces and Films, 1990, 8, 68-72.	2.1	108
146	Heteroepitaxial growth of layered transition metal dichalcogenides on sulfurâ€ŧerminated GaAs{111} surfaces. Applied Physics Letters, 1990, 56, 327-329.	3.3	113
147	Application of Van der Waals epitaxy to highly heterogeneous systems. Journal of Crystal Growth, 1989, 95, 603-606.	1.5	80
148	Characteristic Secondary Electron Emission from Graphite and Glassy Carbon Surfaces. Japanese Journal of Applied Physics, 1988, 27, L759-L761.	1.5	10
149	Low-Energy Electron Energy Loss Spectroscopy on YBa2Cu3O7-y. Japanese Journal of Applied Physics, 1988, 27, L304-L307.	1.5	12